Direct measurement of coherent light proportion from a ~~practical~~ laser~~source~~

Xi Jie Yeo,[1] Eva Ernst,[1] Alvin Leow,[2] Jaesuk Hwang,[1] Lijiong Shen,[1] Peng Kian Tan,[1] and Christian Kurtsiefer[1,2]

[1] *Centre for Quantum Technologies, National University of Singapore, 3 Science Drive 2, Singapore 117543*
[2] *Department of Physics, National University of Singapore, 2 Science Drive 3, Singapore 117551*

(Dated: August 31, 2023)

We present a technique to ~~estimate~~ measure the proportion of ~~coherent emission in the light~~ optical power in the brightest coherent mode emitted by a ~~practical laser source~~light source, without spectral filtering~~, using interferometric photon correlation measurements, where photon correlations are measured between the light emitted from the~~ . This proportion is extracted from correlation of photoevents detected at the output ports of an asymmetric Mach-Zehnder interferometer. Using this technique, we determine the proportion of ~~coherent emission in the light emitted by a laser diode, in a statistical mixture of light from stimulated and spontaneous emission, and a statistical mixture of light from stimulated emission~~ power in the brightest coherent mode of a semiconductor laser, over a range of currents around the threshold current, where a mixture of coherent and incoherent light is expected. We also identified a regime where coherent emission is observed at two distinguishable spectral bands with this technique.

I. INTRODUCTION

~~The invention of lasers can be traced to work describing the emission process of the light from an atom to be spontaneous or stimulated [1]. An ensemble of light emitters undergoing stimulated emission will emit coherent lightthat has a well-defined phase, whereas an ensemble of light emitters undergoing spontaneous emission will emit incoherent light which is randomly phased [2].~~

~~In traditional models of macroscopic lasers [3–5], the light emitted from a laser is modeled to originate dominantly from stimulated emission. These models also predict a phase transition of the nature of emission at the lasing threshold, separating two operating regimes where light emitted is either spontaneous or stimulated.~~

~~However, experiments on small lasers have shown that the transition from spontaneous to stimulated emission is not abrupt, but extends over a range for the pump power [6–10]. Across this range the light emitted from the laser is a mixture of spontaneous and stimulated emission~~The laser has been the workhorse in advancing optical science and engineering over the past decades, providing a source of coherent light [3–5]. Coherent light is at the heart of many applications including interferometry [11], metrology [12], and some quantum key distribution protocols [13, 14].

~~In these experiments, the transition from spontaneous to stimulated emission was characterized~~ A coherent light source can be identified by measuring the ~~second-order photon correlation $g^{(2)}$, which corresponds to the~~ distribution of timing separations between single photon detection events, using the standard Hanbury-Brown and Twiss scheme~~[15]. The measurement result can be explained using Glauber'~~ [15]. According to Glauber's theory of optical coherence~~[16], where incoherent light from spontaneous emission would exhibit a "bunching" signature with $g^{(2)}(0) > 1$, while coherent light from stimulated emission exhibits~~ [16], the timing separation for coherent light follows a Poissonian distribution~~with~~, with a second-order correlation $g^{(2)} = 1$.

~~The "bunching" signature associated with incoherent light has a characteristic timescale inversely related to the spectral width of the light, according to the Wiener-Khintchine theorem related through a Fourier transform [17–19]. In a practical measurement, the amplitude of the~~ However, light emitted by a practical laser source may contain an incoherent component, yet exhibit $g^{(2)} \approx 1$, indistinguishable from coherent light. One example is a laser operating near the lasing threshold, where light emitted is a mixture of coherent and incoherent light [6–10, 20–23]. Although incoherent light can in principle be discerned by its "bunching" signature ~~scales with the ratio of characteristic timescale of the light to the timing response of the detectors [24] . Thus, when the spectral width of the incoherent light is broad , to the extent that the characteristic timescale of the "bunching" signature is smaller than the detector timing uncertainty, incoherent light may~~ $g^{(2)}(0) > 1$, this can be obscured when the incoherent light has a broad spectral width [17–19, 24]. Here, a mixture of coherent and broadband incoherent light would exhibit $g^{(2)} \approx 1$~~, like coherent light~~.

~~To~~ The incoherent component can be spectrally filtered to overcome the limited detector timing ~~uncertainty, a narrow band of incoherent light can be prepared with filters from a wide optical spectrum of an incoherent licht source~~resolution [25]. ~~The narrow spectral width of a filtered incoherent light has a correspondingly larger characteristic coherence timescale, which may be long enough to be resolvable by the detectors.~~

~~However, for characterising the transition from spontaneous to stimulated emission of a laser, such spectral filtering presents some shortcomings. First, as spectral filtering discards~~ However, the light outside the transmission window of a ~~filter, a result would be~~ spectral filter is discarded, and measurements are inconclusive for the full emission of the source. ~~Second~~Furthermore,

spectral filtering ~~requires *a priori* information or an educated guess of the central frequency and bandwidth of stimulated emission. Third, it has been shown that spectral filtering~~ below the Schawlow-Townes linewidth of ~~the~~ a laser result in $g^{(2)}(0) > 1$, ~~similar to light from spontaneous emission [26].~~ suggesting incoherent light emission even if the laser emits coherent light [26].

~~This motivates for methods quantifying the proportion of coherent lightemitted by a source without the need for spectral filtering. A method to characterise the stimulated and spontaneous emission from a pulsed laser has been demonstrated before [23].~~ Another example is a laser in multimode operation [27, 28]. In multimode operation, a laser may emit coherent light in multiple transverse and/or longitudinal modes. The light in each mode may be coherent, but a combination of multiple modes may result in a randomly phased light, and therefore incoherent.

In this paper, we present a method to ~~quantify bounds for~~ measure the proportion of ~~coherent light for a continuous wave laser. Specifically, we investigate the brightest mode of coherent emission from a semiconductor laser diode without spectral filtering, by using~~ optical power in the brightest coherent mode of a laser via the second-order correlation of photodetection events at the output ports of an asymmetric Mach-Zehnder interferometer, also termed interferometric photon correlations. ~~Earlier methods of interferometric photon correlation measurements were used to study spectral diffusion in organic molecules embedded in solid matrix [29, 30]. The method of interferometric photon correlation used in this paper~~ We use this technique to characterise the emission of a diode laser over a wide range of operating currents. Near the lasing threshold, a continuous increase of the coherent light proportion with the operating current is observed. Above the lasing threshold, a multimode operation regime is identified. With further increase of operating current, the proportion of coherent light approaches unity, towards full coherent emission. This technique was originally applied to ~~differentiating between incoherent light and~~ differentiate incoherent light from coherent light with amplitude fluctuations [31]~~. In contrast to second-order photon correlations, this method can clearly distinguish between a~~, and should clearly distinguish finite linewidth coherent light ~~and~~ from broadband incoherent light [32]. ~~We use this method to extract the fraction of coherent light emitted by the laser diode over a range of pump powers across the lasing threshold, and in the lasing regime above threshold where coherent light is emitted into two distinguishable longitudinal modes~~Similar schemes were also used to study spectral diffusion in organic molecules embedded in solid matrix [29, 30].

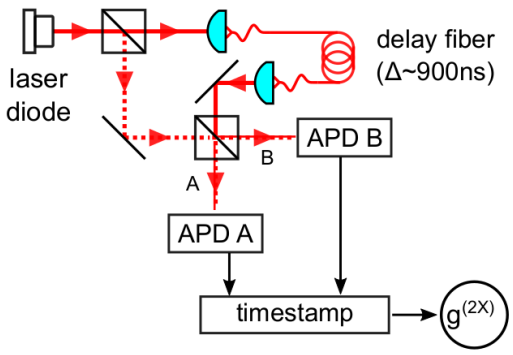

FIG. 1. Experimental setup for measuring interferometric photon correlations. Light from a laser diode enters an asymmetric Mach-Zehnder Interferometer. ~~Singe~~ Single photon avalanche photodetectors (APD) ~~generate photodetection events~~ at each output port of the interferometer generate photodetection events, which are time-stamped to extract the ~~the~~ correlations numerically.

II. INTERFEROMETRIC PHOTON CORRELATIONS

The setup for an interferometric photon correlation measurement $g^{(2X)}$ is shown in Fig. 1. Light emitted by the laser diode is sent through an asymmetric Mach-Zehnder interferometer, with a long propagation delay Δ between the two paths of the interferometer that exceeds the coherence time of the light.

With a light field $E(t)$ at the input, the light fields at the output ports A, B of the interferometer are

$$E_{A,B}(t) = \frac{E(t) \pm E(t+\Delta)}{\sqrt{2}}, \tag{1}$$

with the relative phase shift π acquired by one of the output fields from the beamsplitter.

~~Using these expressions for the electrical fields, the~~ The temporal correlation of photodetection events between the two output ports is given by

$$g^{(2X)}(t_2 - t_1) = \frac{\langle E_A^*(t_1) E_B^*(t_2) E_B(t_2) E_A(t_1)\rangle}{\langle E_A^*(t_1) E_A(t_1)\rangle \langle E_B^*(t_2) E_B(t_2)\rangle}, \tag{2}$$

~~Therein~~therein, $\langle\rangle$ indicates an expectation value~~and/or an ensemble average.~~. Using Eqn. 1, $g^{(2X)}(t_2 - t_1)$ can

be grouped in several terms:

$$
\begin{aligned}
&g^{(2X)}(t_2-t_1) = \\
&= \frac{1}{4}[\langle E^*(t_1)E^*(t_2)E(t_2)E(t_1)\rangle \\
&\quad + \langle E^*(t_1+\Delta)E^*(t_2+\Delta)E(t_2+\Delta)E(t_1+\Delta)\rangle \\
&\quad + \langle E^*(t_1+\Delta)E^*(t_2)E(t_2)E(t_1+\Delta)\rangle \\
&\quad + \langle E^*(t_1)E^*(t_2+\Delta)E(t_2+\Delta)E(t_1)\rangle \\
&\quad - \langle E^*(t_1+\Delta)E^*(t_2)E(t_2+\Delta)E(t_1)\rangle \\
&\quad - \langle E^*(t_1)E^*(t_2+\Delta)E(t_2)E(t_1+\Delta)\rangle]\,.
\end{aligned}
\tag{3}
$$

The first two terms have the form of conventional second-order photon correlation functions $g^{(2)}(t_2-t_1)$. The next two terms are conventional second-order photon correlation functions, time-shifted forward and backward in their argument by the propagation delay Δ in the interferometer. The last two terms have negative signs and reduce $g^{(2X)}$, leading to a dip at ~~zero time difference $t_2 - t_1$~~ zero-time difference $t_2 - t_1 = 0$, with a width given by the coherence time of the light.

The expectation values appearing in Eqn. 3 for $g^{(2X)}$ can be evaluated by using ~~statistical~~ expressions [2] of $E(t)$ for incoherent light and coherent light [32].

For incoherent light, $g^{(2X)}$ exhibits a "bunching" signature peaking at time differences plus and minus the propagation delay, ~~$g^{(2X)}(\pm\Delta) = 1 + 1/4$~~ $g^{(2X)}(\pm\Delta) = 1 + (1/4)$. At zero-time difference, the expected "bunching" signature from conventional second-order photon correlation functions in the first two terms of Eqn. 3 and the dip from the last two terms of Eqn. 3 cancel each other, resulting in $g^{(2X)}(0) = 1$ ~~.~~ (see Fig. 3 top).

For coherent light, since the second-order photon correlation function $g^{(2)}$ has a constant value of 1, the $g^{(2X)}$ will show the negative contributions from the last two terms of Eqn. 3, resulting in $g^{(2X)}(0) = 1/2$ ~~.~~ (see Fig. 3 bottom).

III. EXTRACTING ~~FRACTION~~ PROPORTION OF COHERENT LIGHT~~EMITTED IN A MIXTURE~~

~~In order to~~ To obtain an interpretation of the nature of the light emitted beyond just presenting the components of $g^{(2X)}$, we consider a light field that is neither completely coherent nor incoherent. We assume that light emitted by the laser is a mixture of coherent light field $E_{\rm coh}$, and ~~an uncorrelated~~ a light field $E_{\rm unc}$ ~~, which nature~~ uncorrelated to $E_{\rm coh}$. The nature of $E_{\rm unc}$ can be coherent, incoherent, or a coherent-incoherent mixture. In the following, we try to extract quantitative information about the components from the interferometric photon correlations $g^{(2X)}$, namely the ~~fraction of coherent light intensity of~~ proportion of optical power in the brightest coherent component in the light field, and a collective treatment of all the rest.

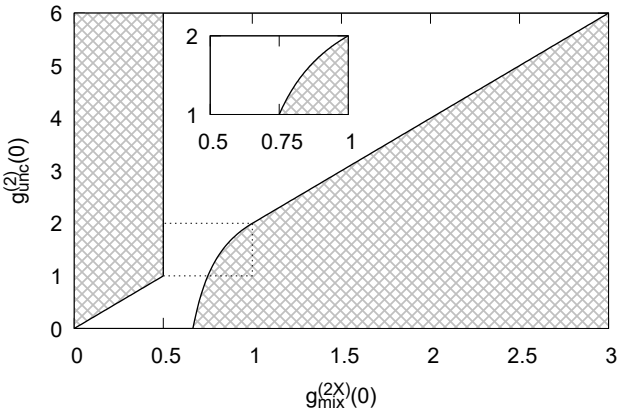

FIG. 2. Combinations of $g^{(2)}_{\rm unc}(0)$ and $g^{(2X)}_{\rm mix}(0)$ that correspond to physical and real-valued ρ. In shaded areas, no such solution exist. Inset: Zoom into the region $1 \le g^{(2)}_{\rm unc}(0) \le 2$, where the uncorrelated light source is assumed to be a mixture of coherent and completely incoherent light, and thermal light.

We model the light field mixture with an electrical field

$$
E_{\rm mix}(t) = \sqrt{\rho}E_{\rm coh}(t) + \sqrt{1-\rho}E_{\rm unc}(t)\,, \tag{4}
$$

where ρ is the ~~fraction of coherent light intensity of~~ proportion of optical power the brightest coherent emission, and the respective light field terms are normalised such that ~~$|E_{\rm res}| = |E_{\rm coh}| = |E_{\rm unc}|$~~ $|E_{\rm mix}| = |E_{\rm coh}| = |E_{\rm unc}|$.

Evaluating photon correlation in Eqn. 3 with this light model, and further assuming that ~~(1)~~ first, the propagation delay in the interferometer is significantly longer than the coherence time scale of the light source, and ~~(2)~~ second, the interferometer has good visibility yields

$$
g^{(2X)}_{\rm mix}(0) = 2\rho - \frac{3\rho^2}{2} + \frac{(1-\rho)^2}{2}g^{(2)}_{\rm unc}(0)\,, \tag{5}
$$

at ~~zero time~~ zero-time difference, with only two remaining parameters, ρ and $g^{(2)}_{\rm unc}(0)$, the ~~zero time~~ zero-time difference second order photon correlation of the uncorrelated field (see Appendix A).

~~The connection in~~ Using Eqn. 5, together with the physical ~~requirement~~ constraint $0 \le \rho \le 1$ for the coherent light ~~fraction~~ proportion limits the possible combinations of $g^{(2)}_{\rm unc}(0)$ and $g^{(2X)}_{\rm mix}(0)$, shown as non-shaded areas in Fig. 2; the exact expressions for the boundaries are given in Appendix B.

We can now further assume that the nature of the uncorrelated light source is some mixture of coherent and completely incoherent light ($g^{(2)}(0) = 1$), and thermal light ($g^{(2)}(0) = 2$). This constrains the second-order photon correlation of the uncorrelated light:

$$
1 \le g^{(2)}_{\rm unc}(0) \le 2. \tag{6}
$$

We impose these bounds in Eqn. 5, and extract the bounds to the ~~fraction of coherent light of~~ proportion of optical power in the brightest coherent emission ρ with an upper bound,

$$\rho \leq \sqrt{2 - 2\, g^{(2X)}(0)}, \tag{7}$$

and a lower bound,

$$\rho \geq \begin{cases} \frac{1}{2} + \frac{1}{2}\sqrt{3 - 4\, g^{(2X)}(0)}, & \text{for } \frac{1}{2} \leq g^{(2X)}(0) \leq \frac{3}{4} \\ 2 - 2\, g^{(2X)}_{\text{mix}}(0), & \text{for } \frac{3}{4} \leq g^{(2X)}(0) \leq 1 \end{cases}, \tag{8}$$

with $g^{(2X)}_{\text{mix}}(0)$ ranging from 1/2 for fully coherent light, to 1 for fully incoherent light.

In practice, these two bounds for ρ are quite tight, and allow to extract a ~~fraction~~ proportion of coherent light in an experiment with a small uncertainty.

IV. EXPERIMENT

In our experiment, we measure interferometric photon correlations of light emitted from a temperature-stabilised distributed feedback laser diode with a central wavelength around 780 nm.

The setup is shown in Fig. 1. Interferometric photon correlations are obtained from an asymmetric Mach-Zehnder interferometer, formed by 50-50 fibre beamsplitters and a propagation delay Δ of about 900 ns through a 180 m long single mode optical fibre in one of the arms. Photoevents at each output port of the interferometer were detected with actively quenched silicon single photon avalanche photo diodes (APD). The detected photoevents were time-stamped using a timetagger with a resolution of 2 ns for an integration time T.

The correlation function $g^{(2X)}$ is extracted through histogramming all time differences $t_2 - t_1$ between detection event pairs in the inverval T numerically~~, which allows for a clean normalization.~~. The resulting correlation is fitted to a two-sided exponential function,

$$g^{(2X)}(t_2 - t_1) = 1 - A \cdot \exp\left(-\frac{|t_2 - t_1|}{\tau_c}\right), \tag{9}$$

where τ_c is the characteristic time constant of the coherent light, and A is the amplitude of the dip. The value of $g^{(2X)}(0)$ is the extracted from the fit as $1 - A$. Examples of measured correlation functions and corresponding fits for different laser powers are shown in Fig. 3.

A. Tranisition from incoherent to coherent light

A transition from incoherent to coherent emission is expected as the laser current is increased across the lasing threshold of the laser. We identify the lasing threshold of a laser diode $I_{L,th}$, by measuring the steepest increase

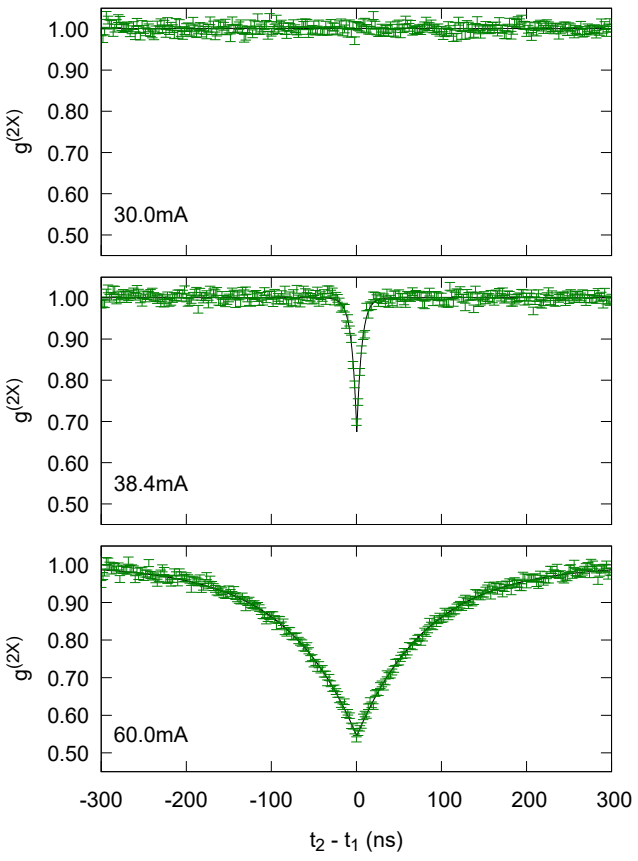

FIG. 3. Interferometric photon correlations $g^{(2X)}$ for different laser currents I_L, extracted from a histogram of photodetector time differences (green symbols). The error range at a specific time bin indicates an expected uncertainty according to a Poissonian counting statistics. The black solid lines show a fit to Eqn. 9, resulting in values for A (from top to bottom) of -0.0006 ± 0.0003, 0.326 ± 0.008, 0.455 ± 0.002, respectively.

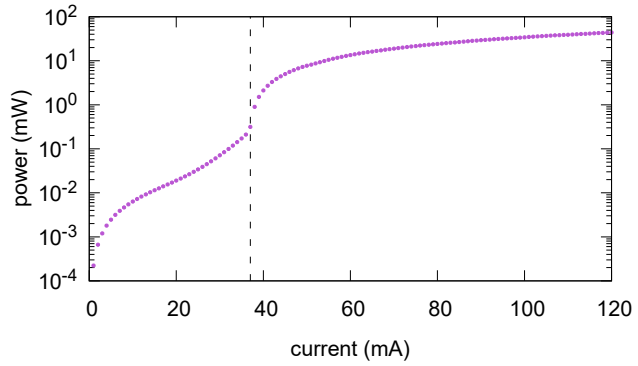

FIG. 4. Measured laser power against laser current I_L. The sharpest change in current was measured at $I_{L,th} = 37$ mA, indicating the threshold current (dashed line).

of optical power with the laser current (see Fig 4). For our diode, we find $I_{L,th} = 37\,\mathrm{mA}$.

To observe the transition from incoherent to coherent emisssion, we measure the ~~fraction of coherent light intensity of~~ proportion of optical power in the brightest coherent component ~~in the light field~~ ρ , at different laser current I_L across the lasing threshold, extracted from $g^{(2X)}$ measurements. The interferometric photon correlation measurements as a function of the laser current ~~around the lasing threshold~~ are shown in Fig. 5 (top part). The amplitude of the dip is then extracted by fitting these ~~measurements~~ correlations to Eqn. 9, from which the upper bound and lower bound of ~~the fraction of coherent light from the most dominant coherent emission~~ ρ is extracted (see Fig. 5, middle part).

From the fit, the ~~fraction ρ of coherent emission~~ proportion of coherent light ρ remains near 0 when operated below threshold. Above the lasing threshold at 37 mA, ρ increases with I_L in a phase-transition manner, reaching $\rho = 0.986$ (90% confidence interval: 0.982 to 0.989) at $I_L = 120\,\mathrm{mA}$. This agrees with the expectation that the emission of the laser diode is increasingly dominated by stimulated emission past the lasing threshold[33, 34].

Near the lasing threshold, a tight upper and lower bound of ρ is observed, in agreement with the expectation that emission of light with a ~~statistical~~ mixture of coherent and incoherent light from the laser diode is expected when operating it near its lasing threshold [33, 34].

The coherence time of the coherent light τ_c can also be extracted from fitting $g^{(2X)}$ measurements to Eqn. 9 (bottom Fig. 5). We observe that the coherence time increases with the current after the threshold current, before reaching a steady value between 300 to 350 ns. The increase of coherence time correspond to a narrowing of the emission linewidth, agrees with predictions from laser theory, that line narrowing is expected with an increase in pumping of the laser (here an increase in laser current)[34]. An oscillation of the coherence time is also observed starting at ~~the about~~ 66 mA, with a periodicity of about 6 mA.

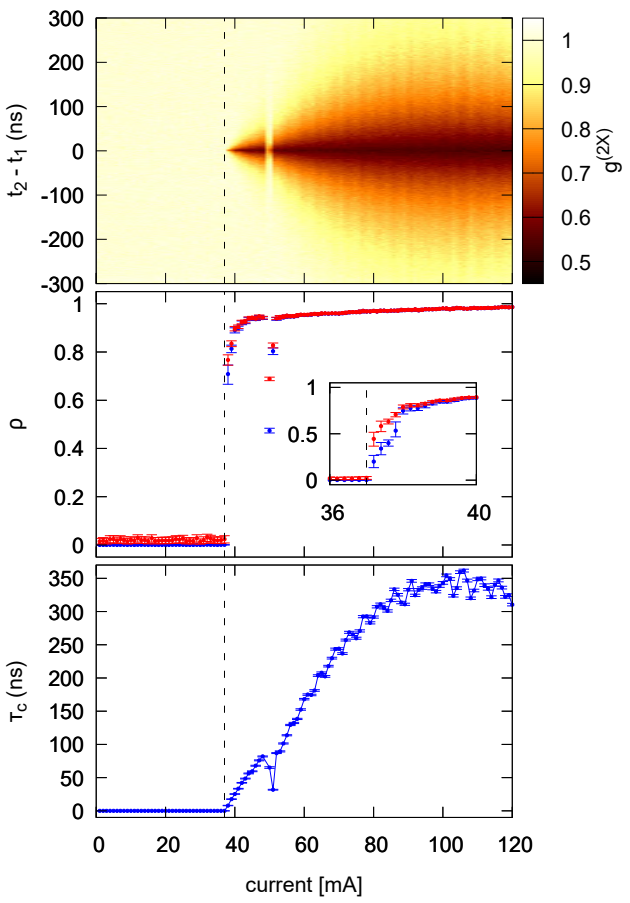

FIG. 5. Top: Interferometric photon corrrelations $g^{(2X)}$ for different ~~drive~~ operating currents I_L. Middle: Corresponding upper bound of ~~fraction~~ proportion ρ of coherent light (red) extracted via Eqn. C1, and the lower bound (blue) extracted via Eqn. C2 from $g^{(2X)}(0)$. The dip in ρ is a result of emission at multiple ~~chop~~ chip modes as explained in Section IV B. The inset shows the extracted bounds for ρ at finer steps of laser current near the lasing threshold. Bottom: Coherence time of coherent light τ_c extracted from $g^{(2X)}$. The dashed line indicates the threshold current $I_{L,th} = 37\,\mathrm{mA}$.

B. Light statistics near a mode hop

Above the lasing threshold, the laser oscillates at different longitudinal modes for different laser currents. The technique to extract the ~~fraction of coherent and incoherent light allows to investigate the behavior also in the transition regime between~~ proportion of coherent light also allows investigation on the behaviour in the regime where oscillation on different longitudinal lasing modes is observed.

~~For this, we~~ In measuring the proportion of coherent light ρ for different operating currents, we observed a reduction in ρ over a range of currents above the lasing threshold (Fig. 5 middle). To further investigate, we measured the spectrum of light emitted by the laser diode ~~at different currents above the lasing threshold~~ over this range of currents with an optical spectrum analyser based on a Michelson interferometer with a spectral resolution of 2 GHz (Bristol 771B-NIR). ~~The laser diode emitted light into two distinct narrow spectral bands with a changing power ratioin a diode current range between~~ At laser currents between 49.0 mA and 52.4 ~~mA~~mA, two distinct narrow spectral bands of light were emitted by the laser diode with a varying power ratio, suggesting emission in two chip modes. Outside this window, only one of the modes was present. Below 49.0 mA, the laser emission was centered around 780.07 nm, above 52.4 mA around 780.34 nm,

The power fractions $r_{\alpha,\beta}$ of these two chip modes α and β emitting respectively at powers $P_{\alpha,\beta}$ near this transi-

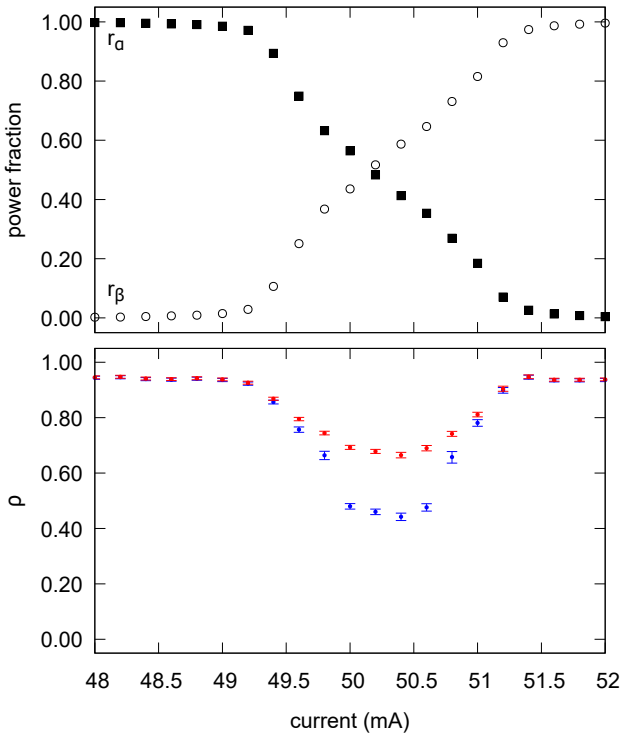

FIG. 6. Different chip modes of the laser diode are excited for different currents, resulting in a reduction of the $g^{(2X)}$ signature in a mode competition regime. Top: Power ratios $r_{\alpha,\beta}$ as a function of current for the chip modes α and β emitting in narrow bands around 780.07 nm (solid squares) and 780.34 nm (hollow circles), respectively. Bottom: Upper bound of ~~fraction~~ proportion ρ of coherent light (red) extracted via Eqn. C1, and the lower bound (blue) extracted via Eqn. C2 from $g^{(2X)}(0)$.

tion,

$$r_{\alpha,\beta} = \frac{P_{\alpha,\beta}}{P_\alpha + P_\beta}\,, \tag{10}$$

undergo a ~~nearly linear transition~~ transition from a chip mode with emission wavelength centered around 780.07 nm to another chip mode with centered around 780.34 nm (see top traces of Fig. 6).

We measured $g^{(2X)}$ in the same transition regime ~~and extract~~ at finer current steps and extracted the proportion of coherent light from the ~~most dominant~~ brightest coherent emission ρ as described above (see Fig. 6, bottom trace). In the transition regime, the ~~fraction~~ proportion ρ of coherent emission extracted ~~this way~~ from $g^{(2X)}$ decreases, when there is emission at multiple chip modes, and increases again when the emission approaches a single chip mode. ~~This~~ Based on our model of the light field in Eqn. 4, this can be interpreted as the light of one emission band being uncorrelated to the light of the other emission band, although the light in each band is coherent with itself.

V. CONCLUSION

We presented a method to extract the proportion of coherent light emitted by a laser diode without the use of spectral filters, using interferometric photon correlations. As a demonstration, we measured interferometric photon correlations of light emitted from a laser diode over a range of operating currents~~near the lasing threshold,~~ , and extracted the proportion of ~~coherent light~~ light intensity emitted from the brightest coherent emission, showing an increase in proportion of coherent light emission as the operating current was increased past the lasing threshold. We also used this technique to characterize the coherence of emission in a ~~transition regime~~ mode hop between longitudinal modes above the lasing threshold, and find a reduction of the ~~fraction~~ proportio of coherent light there, suggesting that the two longitudinal modes can be viewed as independent and mutually incoherent coherent emissions. Apart from the characterisation of lasers, this method may also be useful in practical applications of some continuous-variable quantum key distribution protocols ~~[13, 14]~~, where the noise of a coherent state source such as a laser, may need to be characterised [35–37].

Appendix A: Interferometric photon-correlation for a mixture of light fields

We show here in further detail the derivation of Eqn.5, by calculating the interferometric photon correlation using the model light field in Eqn. 4.

The evaluation of $g^{(2X)}$ via Eqn. 3 requires the conventional second-order photon correlation function ~~$g^{(2)}(t_1 - t_2) = \langle E^*(t_1)E^*(t_2+\Delta)E(t_2)E(t_1+\Delta)\rangle$~~$g^{(2)}(t_1 - t_2) = \langle E$ and the last ~~terms (CK: how many?)~~two terms in Eqn. 3 containing negative signs. For the light field mixture Eqn. 4, its conventional second-order photon correlation function is given by

$$\begin{aligned} g^{(2)}_{\rm mix}(t_2 - t_1) = \\ =&\rho^2\, g^{(2)}_{\rm coh}(t_2 - t_1) + (1-\rho)^2\, g^{(2)}_{\rm unc}(t_2 - t_1) \\ &+ 2\rho(1-\rho)\left[1 + \Re[g^{(1)}_{\rm coh}(t_2 - t_1)\, g^{(1)*}_{\rm unc}(t_2 - t_1)\right] \end{aligned}\,, \tag{A1}$$

where $g^{(1)}$ is the first-order field correlation function for the respective component light fields, $g^{(1)*}$ its complex conjugate, and $\Re[\cdots]$ extracts the real part of its argument.

The last terms in Eqn. 3 can be written as

$$\begin{aligned} &\langle E^*_{\rm mix}(t_1)E^*_{\rm mix}(t_2+\Delta)E_{\rm mix}(t_2)E_{\rm mix}(t_1+\Delta)\rangle \\ =&\rho^2\,|g^{(1)}_{\rm coh}(t_2 - t_1)|^2 + (1-\rho)^2|g^{(1)}_{\rm unc}(t_2 - t_1)|^2 \\ &+2\rho(1-\rho)\,\Re[g^{(1)}_{\rm coh}(t_2 - t_1)\, g^{(1)*}_{\rm unc}(t_2 - t_1)] \\ &+2\rho(1-\rho)\,\Re[g^{(1)}_{\rm coh}(\Delta)\, g^{(1)*}_{\rm unc}(\Delta)] \end{aligned}\,, \tag{A2}$$

where $g^{(1)}(\Delta) \approx 0$ for our experimental situation of the propagation delay Δ significantly larger than the coherence times of the respective light sources. Note that all terms in Eqn. A2 are real-valued.

With this, the interferometric photon correlation at ~~zero time~~ zero-time difference is given by

$$\begin{aligned} g^{(2X)}_{\mathrm{mix}}(0) &= \\ &= \frac{1}{4}[g^{(2)}_{\mathrm{mix}}(\Delta) + g^{(2)}_{\mathrm{mix}}(-\Delta) \\ &\quad + 2(\rho^2\, g^{(2)}_{\mathrm{coh}}(0) + (1-\rho)^2\, g^{(2)}_{\mathrm{unc}}(0) + 2\rho(1-\rho)) \\ &\quad - 2(\rho^2\, |g^{(1)}_{\mathrm{coh}}(0)|^2 + (1-\rho)^2 |g^{(1)}_{\mathrm{unc}}(0)|^2)]\,. \end{aligned} \tag{A3}$$

We make further assumptions that the propagation delay in the interferometer Δ is significantly longer than the coherence time scale of the light source, such that $g^{(2)}_{\mathrm{mix}}(\pm\Delta) \approx 1$, the interferometer has good visibility, such that ~~$g^{(1)}(0) \approx 1$~~$|g^{(1)}(0)| \approx 1$, and for the second order photon correlation of the coherent light field is $g^{(2)}_{\mathrm{coh}}(0) = 1$. The evaluation of these assumptions in Eqn. A3 leads to the relationship shown in Eqn. 5.

Appendix B: Boundaries of physically meaningful combinations of interferometric correlations in a mixture

Assuming a binary mixture of the light field as per Eqn. 4, the interferometric correlation of the mixture, $g^{(2X)}_{\mathrm{mix}}(0)$, and the conventional second order correlation of the incoherent light, $g^{(2)}_{\mathrm{unc}}(0)$, at zero time difference are constrained by relation Eqn. 5. Further assuming the physical requirement $0 \le \rho \le 1$ for the coherent light ~~fraction~~ proportion gives a lower bound for $g^{(2)}_{\mathrm{unc}}(0)$,

$$g^{(2)}_{\mathrm{unc}}(0) \ge \begin{cases} 0\,, & g^{(2X)}_{\mathrm{mix}}(0) \le \frac{2}{3} \\ 3 + \frac{1}{1-2g^{(2X)}_{\mathrm{mix}}(0)}, & g^{(2X)}_{\mathrm{mix}}(0) \in [\frac{2}{3}, 1] \\ 2g^{(2X)}_{\mathrm{mix}}(0) & g^{(2X)}_{\mathrm{mix}}(0) \ge 1 \end{cases}. \tag{B1}$$

For $g^{(2X)}_{\mathrm{mix}}(0) \in [0, \frac{1}{2})$, there is an upper bound for $g^{(2)}_{\mathrm{unc}}(0)$,

$$g^{(2)}_{\mathrm{unc}}(0) \le 2g^{(2X)}_{\mathrm{mix}}(0)\,. \tag{B2}$$

Appendix C: Error propagation from fitting of $g^{(2X)}$ measurement

Standard techniques in propagation of uncertainties are not used, as the expressions in Eqn. 7-8 would lead to indefinite values of uncertainties at some values of A. We thus extract the upper and lower bounds of ρ by performing a change in variables from the probability density of A.

The probability density of A is assumed to be a normal distribution with a mean value and standard deviation respectively the value and uncertainty of A extracted from the curve fitting of $g^{(2X)}$ to Eqn. 9.

The probability densities describing the upper and lower bounds of ρ is obtained from a change of variable from A by rewriting Eqn. 7-8 in terms of A. The ~~transfomation~~ transformation of the upper bound is

$$\rho = \sqrt{2A}, \tag{C1}$$

and the lower bound,

$$\rho = \begin{cases} 2A, & \text{for } 0 \le A \le \frac{1}{4} \\ \frac{1}{2} + \frac{1}{2}\sqrt{4A-1}, & \text{for } \frac{1}{4} \le A \le \frac{1}{2} \end{cases}. \tag{C2}$$

We exclude non-physical values of ρ by setting the probability density outside the domain $0 \le \rho \le 1$ to 0~~, to 0.~~. The probability density is renormalised by dividing over its integral. From these probability densities of the upper bound and lower bound of ρ, we compute the expectation of ρ and its 90% confidence interval, which would be reported respectively as the data points and errorbars in plots which contains measurements of ρ.

[1] A. Einstein, Strahlung-emission und-absorption nach der quantentheorie, Verh. d. Deutsche Physik. Ges. **18**, 318 (1916).

[2] R. Loudon, *The Quantum Theory of Light* (Oxford, UK, 2000).

[3] W. E. Lamb, Theory of an optical maser, Phys. Rev. **134**, A1429 (1964).

[4] F. Arecchi and R. Bonifacio, Theory of optical maser amplifiers, IEEE Journal of Quantum Electronics **1**, 169 (1965).

[5] H. Haken, Cooperative phenomena in systems far from thermal equilibrium and in nonphysical systems, Rev. Mod. Phys. **47**, 67 (1975).

[6] Y.-S. Choi, M. T. Rakher, K. Hennessy, S. Strauf, A. Badolato, P. M. Petroff, D. Bouwmeester, and E. L. Hu, Evolution of the onset of coherence in a family of photonic crystal nanolasers, Applied Physics Letters **91**, 031108 (2007).

[7] S. M. Ulrich, C. Gies, S. Ates, J. Wiersig, S. Reitzenstein, C. Hofmann, A. Löffler, A. Forchel, F. Jahnke, and P. Michler, Photon statistics of semiconductor microcavity lasers, Phys. Rev. Lett. **98**, 043906 (2007).

[8] J. Wiersig, C. Gies, F. Jahnke, M. Aßmann, T. Berstermann, M. Bayer, C. Kistner, S. Reitzenstein, C. Schneider, S. Höfling, A. Forchel, C. Kruse, J. Kalden, and D. Hommel, Direct observation of correlations between individual photon emission events of a microcavity laser, Nature **460**, 245–249 (2009).

[9] R. Hostein, R. Braive, L. L. Gratiet, A. Talneau, G. Beaudoin, I. Robert-Philip, I. Sagnes, and A. Beveratos, Demonstration of coherent emission from high-β photonic crystal nanolasers at room temperature, Opt.

Lett. **35**, 1154 (2010).
[10] S. Kreinberg, W. W. Chow, J. Wolters, C. Schneider, C. Gies, F. Jahnke, S. Höfling, M. Kamp, and S. Reitzenstein, Emission from quantum-dot high-ßmicrocavities: Transition from spontaneous emission to lasing and the effects of superradiant emitter coupling, Light: Science & Applications **6**, 10.1038/lsa.2017.30 (2017).
[11] P. Hariharan, *Basics of Interferometry* (Elsevier Academic Press, Amsterdam, Netherlands, 2007).
[12] D. L. Wright, Laser metrology, Developments in Laser Technology I 10.1117/12.946865 (1969).
[13] J. Lodewyck, T. Debuisschert, R. Tualle-Brouri, and P. Grangier, Controlling excess noise in fiber-optics continuous-variable quantum key distribution, Phys. Rev. A **72**, 050303 (2005).
[14] C. Weedbrook, S. Pirandola, R. García-Patrón, N. J. Cerf, T. C. Ralph, J. H. Shapiro, and S. Lloyd, Gaussian quantum information, Rev. Mod. Phys. **84**, 621 (2012).
[15] R. Hanbury-Brown and R. Q. Twiss, Correlation between photons in two coherent beams of light, Nature **177**, 27–29 (1956).
[16] R. J. Glauber, The quantum theory of optical coherence, Phys. Rev. **130**, 2529 (1963).
[17] N. Wiener, Generalized harmonic analysis, Acta Mathematica **55**, 117–258 (1930).
[18] A. Khintchine, Korrelationstheorie der stationären stochastischen prozesse, Mathematische Annalen **109**, 604–615 (1934).
[19] L. Mandel and E. Wolf, *Optical Coherence and Quantum Optics* (Cambridge, UK, 1995).
[20] R. Jin, D. Boggavarapu, M. Sargent, P. Meystre, H. M. Gibbs, and G. Khitrova, Photon-number correlations near the threshold of microcavity lasers in the weak-coupling regime, Phys. Rev. A **49**, 4038 (1994).
[21] S. Strauf, K. Hennessy, M. T. Rakher, Y.-S. Choi, A. Badolato, L. C. Andreani, E. L. Hu, P. M. Petroff, and D. Bouwmeester, Self-tuned quantum dot gain in photonic crystal lasers, Phys. Rev. Lett. **96**, 127404 (2006).
[22] S. H. Pan, Q. Gu, A. El Amili, F. Vallini, and Y. Fainman, Dynamic hysteresis in a coherent high-β nanolaser, Optica **3**, 1260 (2016).
[23] A. George, A. Bruhacs, A. Aadhi, W. E. Hayenga, R. Ostic, E. Whitby, M. Kues, Z. M. Wang, C. Reimer, M. Khajavikhan, and R. Morandotti, Time-resolved second-order coherence characterization of broadband metallic nanolasers, Laser & Photonics Reviews **15**, 2000593 (2021).
[24] D. B. Scarl, Measurements of photon correlations in partially coherent light, Phys. Rev. **175**, 1661 (1968).
[25] P. K. Tan and C. Kurtsiefer, Temporal intensity interferometry for characterization of very narrow spectral lines, Monthly Notices of the Royal Astronomical Society **469**, 1617 (2017).
[26] R. Centeno Neelen, D. M. Boersma, M. P. van Exter, G. Nienhuis, and J. P. Woerdman, Spectral filtering within the schawlow-townes linewidth of a semiconductor laser, Phys. Rev. Lett. **69**, 593 (1992).
[27] H. P. Weber and H. G. Danielmeyer, Multimode effects in intensity correlation measurements, Phys. Rev. A **2**, 2074 (1970).
[28] J. Yin, S. Zhu, W. Gao, and Y. Wang, Second-order coherence g (2) (τ) and its frequency-dependent characteristics of a two-longitudinal-mode laser, Appl Phys B **64**, 65–72 (1996).
[29] X. Brokmann, M. Bawendi, L. Coolen, and J.-P. Hermier, Photon-correlation fourier spectroscopy, Optics Express **14**, 6333 (2006).
[30] L. Coolen, X. Brokmann, and J.-P. Hermier, Modeling coherence measurements on a spectrally diffusing single-photon emitter, Phys. Rev. A **76**, 033824 (2007).
[31] A. Lebreton, I. Abram, R. Braive, I. Sagnes, I. Robert-Philip, and A. Beveratos, Unequivocal differentiation of coherent and chaotic light through interferometric photon correlation measurements, Physical Review Letters **110**, 163603 (2013).
[32] A. Lebreton, I. Abram, R. Braive, I. Sagnes, I. Robert-Philip, and A. Beveratos, Theory of interferometric photon-correlation measurements: Differentiating coherent from chaotic light, Phys. Rev. A **88**, 013801 (2013).
[33] H. Haug and H. Haken, Theory of noise in semiconductor laser emission, Zeitschrift für Physik A Hadrons and nuclei **204**, 262–275 (1967).
[34] H. Haken, *Light: Laser light dynamics* (North-Holland Physics Publishing, Amsterdam, Netherlands, 1981).
[35] Y. Shen, J. Yang, and H. Guo, Security bound of continuous-variable quantum key distribution with noisy coherent states and channel, Journal of Physics B: Atomic, Molecular and Optical Physics **42**, 235506 (2009).
[36] V. C. Usenko and R. Filip, Feasibility of continuous-variable quantum key distribution with noisy coherent states, Phys. Rev. A **81**, 022318 (2010).
[37] Y. Shen, X. Peng, J. Yang, and H. Guo, Continuous-variable quantum key distribution with gaussian source noise, Phys. Rev. A **83**, 052304 (2011).